Long term comparison of spinner anemometer and nacelle lidar data for an offshore wind farm

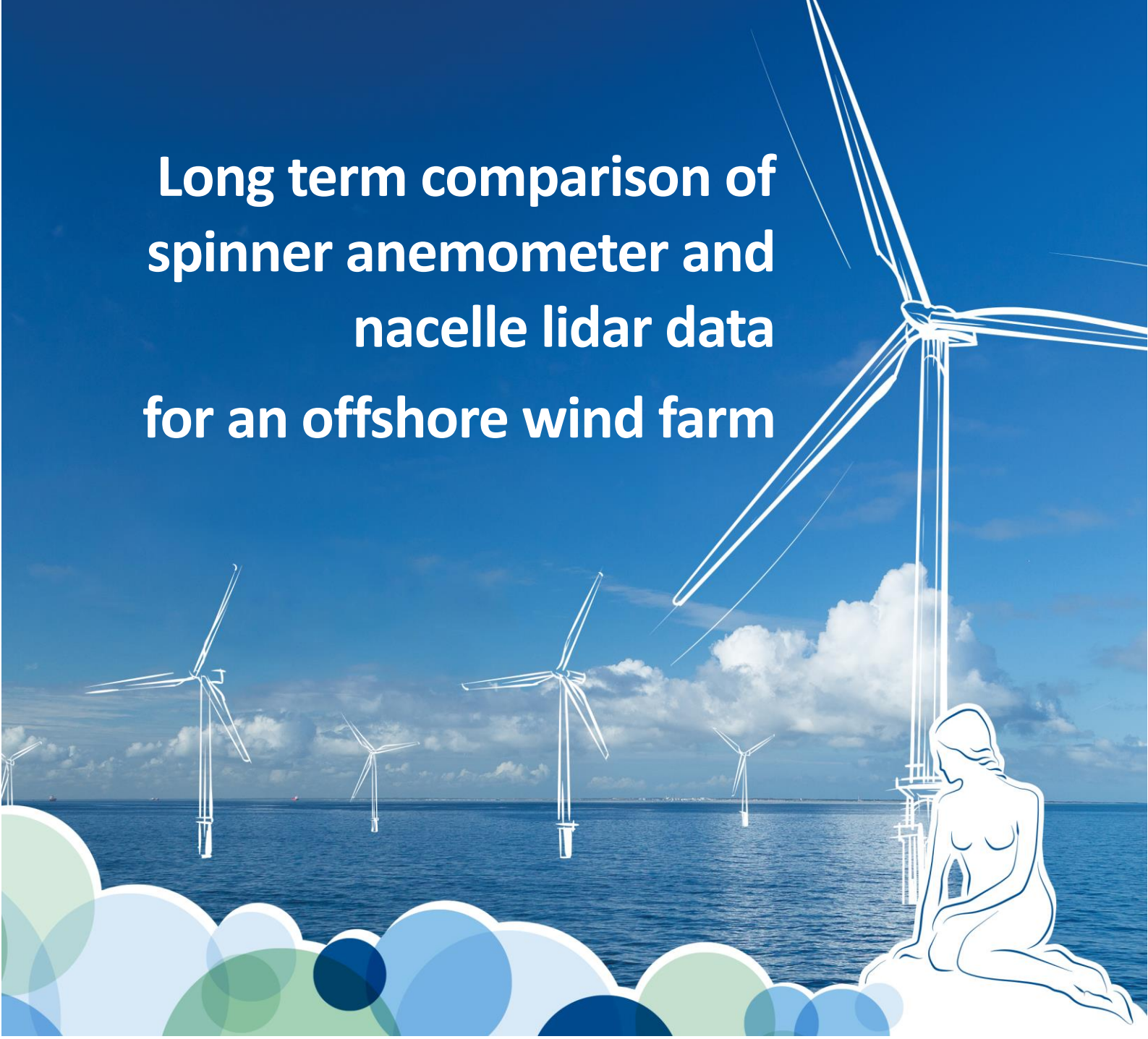

AUTHORS

Katrin Ritter, ROMO Wind, kri@romowind.com
Paula Gómez Arranz, DTU Wind Energy, paar@dtu.dk

Wind EUROPE OFFSHORE 2019
26-28 NOVEMBER
COPENHAGEN

EVENT AMBASSADORS:

MHI VESTAS OFFSHORE WIND · Ørsted · Van Oord Marine ingenuity

IN COLLABORATION WITH:

SUMMARY

The “spinner anemometer” is an instrument installed on a wind turbine spinner that measures wind inflow angles and horizontal wind speed in the centre of the turbine rotor. Since it measures inside the turbine induction zone, it requires a STF (Spinner Transfer Function) to obtain the “free wind speed” (i.e. a wind speed that, ideally, is not affected by the flow distortion caused by the wind turbine), which is the input to power curves and Annual Energy Production (AEP) calculations.

The Performance Transparency Project (PTP), funded by EUDP (project partners ROMO Wind and DTU Wind Energy), aims to demonstrate the seasonal and terrain wise robustness of the STF in different terrains and turbine types

PTP has produced more than one year of data from one nacelle lidar and iSpin® (spinner anemometer produced by Romo Wind) in an offshore wind farm. This work presents the preliminary results, where we investigated the seasonal stability of the spinner anemometer wind speed and STF.

In this work we:

- analysed the stability, over fourteen months, of the spinner anemometer wind speed measurements and AEPs and compared them to the ones from a nacelle lidar and a nacelle anemometer,
- performed an AEP uncertainty evaluation for the iSpin and the nacelle lidar,
- investigated the seasonality of the STF, by evaluating the differences in AEP obtained from the application of STFs obtained in one year and in shorter periods, in different seasons (spring, summer, autumn and winter).

METHODOLOGY

The dataset consisted of ten-minute data from iSpin, lidar (WindIris v2) and wind turbine SCADA, from the period February 2018 to May 2019. In the first part of the analysis, we calibrated the spinner anemometer data with a STF and a k_1 factor [1,2] obtained from the (filtered) data in that period. The wind speed differences, power curves, and AEPs from iSpin, nacelle anemometer (SCADA), and lidar were obtained for the full period and for two-month sub-sets. The purpose was to analyse the stability of the spinner anemometer wind speed measurements with respect to the lidar and the nacelle anemometer.

In the second part, we generated STFs and k_1 factors from four shorter periods, and compared these "season" STFs to the previous STF. We also compared the AEPs obtained on a bi-monthly basis from these five STFs. The purpose was to investigate the seasonality of the STF.

1.1. DATA SELECTION

The following filters were applied to select the dataset for the analysis:

- iSpin data quality flag "dataOK" equal to True.
- Lidar data quality flag "Availability" equal to 100%.
- Lidar CNR lower than -5dB for all Lines-of-Sight (LOS); selected based on a note from the manufacturer for this specific unit and firmware version.
- Difference between CNR from top and low LOS lower than 5dB. I.e. $|CNR_0\text{-}CNR_2| < 5dB$ and $|CNR_1\text{-}CNR_3| < 5dB$. In order to exclude extreme events where a fog layer would affect only top or bottom LOS measurements, which may produce an incorrect wind speed.
- Turbine in operation: angular rotor speed > 5 rad/s
- Wind direction between 155° and 300°.

The measurement sector selection was verified by analysing the lidar LOS turbulence and relative wind direction with respect to wind direction [3]. We did not find any indication of wakes from neighbouring turbines.

1.2. STF (SPINNER TRANSFER FUNCTION)

Several STFs were generated from different data periods, following the procedure in [4] but using the nacelle lidar wind speed as the reference (ws_{ref}) instead of a mast-mounted cup anemometer. In each case, we performed the self-consistency test prescribed in Annex D.8 of [4], and selected STFs that fulfilled the pass criteria.

STF_1 was obtained from the full dataset; STF_2 … STF_5, were obtained from two-month periods. Table 1 summarizes the start and end of the selected periods, the number of data, and the k_1 calibration factors. Figure 1 shows the dataset used for STF_1 and illustrates the effect of the STF and k_1 calibrations.

Table 1 STFs periods, number of data after filtering, and k_1 calibration factors.

	Measurement period	Number of data	k1
STF_1 ("year")	10 Feb'18 – 01 May'19	16859	0.69
STF_2 ("spring")	01 Mar'18 – 01 May'18	2340	0.69
STF_3 ("summer")	01 Jul'18 – 01 Sep'18	1929	0.68
STF_4 ("autumn")	01 Sep'18 – 01 Nov'18	3304	0.69
STF_5 ("winter")	01 Nov'18 – 01 Jan'19	1981	0.69

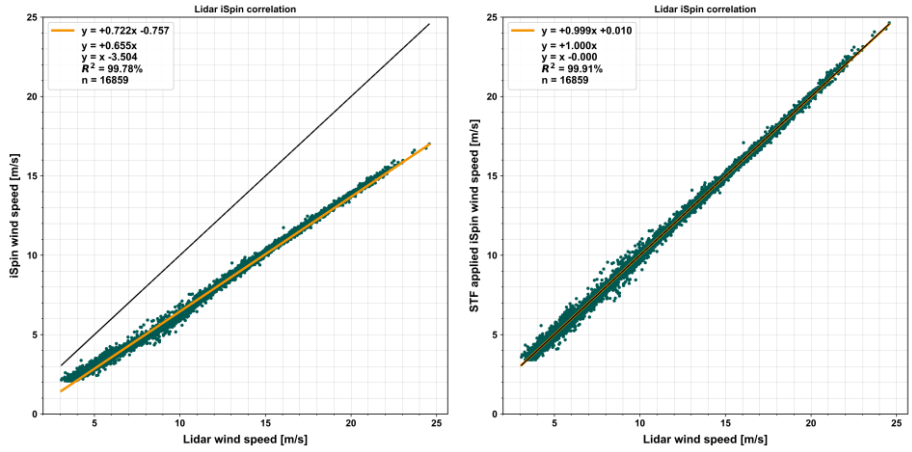

Figure 1 STF_1 dataset: Spinner anemometer speed before applying STF and k_1 (left), and after applying STF and k_1 (right), versus lidar wind speed.

1.3. WIND SPEED DEVIATION

We defined the wind speed deviation (Δws), for each ten-minute dataset as:

$$\Delta ws_x = \frac{ws_x - ws_{ref}}{ws_{ref}} \cdot 100\%$$

where ws_{ref} is the lidar wind speed, and ws_x stands for the spinner anemometer wind speed, ws_{iSpin}, or the nacelle anemometer wind speed (from SCADA), ws_{nac}.

1.4. UNCERTAINTY ASSESSMENT

The uncertainties of the lidar and spinner anemometer one-year power curves, and their AEPs, were calculated based on [5]. The lidar uncertainties were determined following the present IEC draft for the use of nacelle-mounted lidars for wind speed measurements [3].

The spinner anemometer uncertainties were assessed according to [4]; the inputs and uncertainty method were described in [6]. Where available, the input values for the assessment were taken from calibration certificates and installation documents. In other cases, we assumed typical values, based on our experience or common practice. The lidar calibration uncertainty was based on a preliminary test before the installation offshore. This value will be revised after a calibration of all LOS is performed at the end of the project.

Table 2 Summary of power curve uncertainty components and input values for the assessment. Values indicated with (*) are assumptions.

Wind speed uncertainty: $u_{V,i} = \sqrt{u_{VS,i}^2 + u_{terr,i}^2 + u_{M,i}^2}$	
Instrument uncertainty, $u_{VS,i}$	
Lidar [3]	Spinner anemometer [6]
$u_{v_{h,WFR,inputs,i}} \approx \frac{u_{Vlos,3}}{\cos\frac{\alpha_H}{2}\cos\frac{\beta_V}{2}} = 0.12\ m/s$	Calibrations: • Wind tunnel calibrations: $u_{N1,V1,i} = 0.0052V_{1,i} + 0.012\frac{m}{s}$; $u_{N1,V2,i} = 0.0053V_{2,i} + 0.010\frac{m}{s}$; $u_{N1,V3,i}$=$0.0050V_{3,i} + 0.017m/s$ • Angular calibration: $0.1k_\alpha$
$u_{v_{h,operational,i}} \approx 0$	Operational characteristics: class A
$u_{v_{h,WFR,internal,i}} \approx 0$	Sensor mounting: • Longitudinal position: 1 cm • Directional uncertainty: 2° • Sonic path angle deviation: 1° • Sonic azimuth position: 1 cm • Accelerometer alignment: 5° (*)
$u_{vh,measH} = \left(\frac{\left(\frac{z_{hub}+u_z}{z_{hub}}\right)^s - 1}{\sqrt{3}}\right)V_i$	Other: • Data acquisition: 0.006m/s
Flow distortion due to terrain, $u_{terr,i} = 1\%V_i$	
Method uncertainty, $u_{M,i} = \sqrt{u_{M,AD,i}^2 + u_{M,shear-veer,i}^2 + u_{M,upflow,i}^2 + u_{M,sfx,i}^2 + u_{M,TInorm,i}^2 + u_{M,CC,i}^2}$	
Lack of shear and veer normalization: $u_{M,shear-veer,i} = 0.5\%$ (*) Other ≈ 0	
Electrical power uncertainty:	

$$u_{P,i} = \sqrt{u_{P,CT,i}^2 + u_{P,PT,i}^2 + u_{dP,i}^2} = \sqrt{\left(\frac{0.005}{\sqrt{3}} \cdot P_i\right)^2 + \left(\frac{0.0075}{\sqrt{3}} \cdot 1.4P_{nom}\right)^2} (*)$$

Air temperature uncertainty: $u_{T,i} = \sqrt{u_{T,cal,i}^2 + u_{T,shield,i}^2 + u_{T,mnt,i}^2 + u_{dT,i}^2} = 0.5°C(*)$

Air temperature uncertainty: $u_{B,i} = \sqrt{u_{B,cal,i}^2 + u_{B,mnt,i}^2 + u_{dB,i}^2}$=0.6hPa(*)

Relative humidity uncertainty: $u_{RH,i} = \sqrt{u_{RH,cal,i}^2 + u_{RH,mnt,i}^2 + u_{dRH,i}^2} = 0.5\%(*)$

RESULTS

1.5. ONE-YEAR STF

1.5.1. WIND SPEED DEVIATION

The dataset was divided in fourteen two-month subsets. For each subset, we calculated the averages of Δws_{iSpin} and Δws_{nac} (defined in section 1.3). The results are shown in Figure 2. The values in the x-axis indicate the start of each two-month period, e.g. "2018-06" represents data from the 1st of June 2018 to the 31st of July 2018. The box plots indicate the minimum, first quartile, median, third quartile and maximum of Δws_{iSpin} and Δws_{nac} in each period. The distribution of the iSpin - lidar wind speed deviation presents the medians, Q1 and Q3 within ±2%ws_{ref} in all periods.

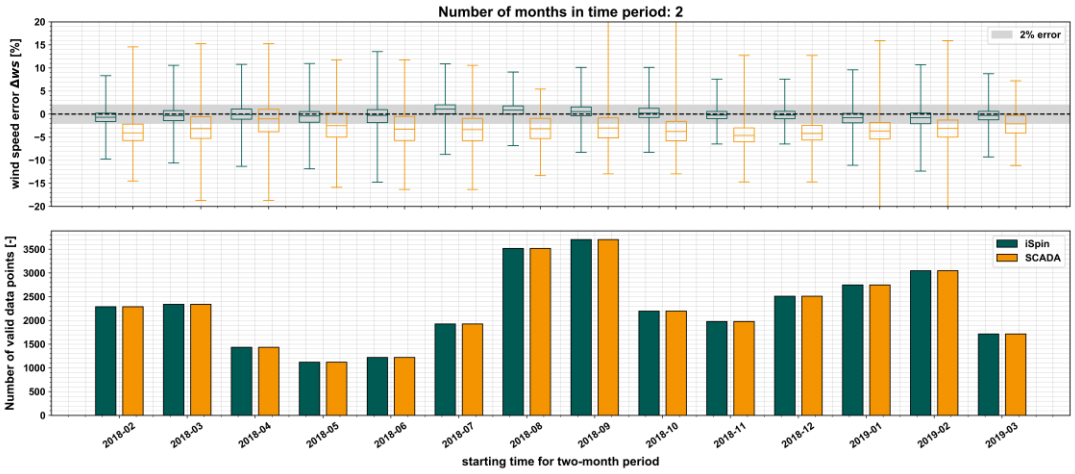

Figure 2 Wind speed deviation distribution (top) and number of data (bottom) for iSpin® and nacelle anemometer (SCADA) in fourteen two-month periods.

1.5.2. AEP COMPARISON

For each two-month dataset, we obtained the power curves from iSpin®, lidar and SCADA wind speeds, and calculated the corresponding AEPs. All power curves were normalized to standard sea level air density and fulfilled the completeness requirements in [5], with the exception that the bins 3 m/s (cut-in) and lower were incomplete in some cases.

The results are shown in Figure 3. A Rayleigh PDF with annual average wind speed of 8m/s was used. Each dot represents the AEP calculated from the iSpin, lidar and nacelle anemometer (SCADA) power curves in each period. The AEP values are normalized to the AEP obtained from the one-year lidar power curve, $AEP_{lidar,1}$. The light grey band indicates the AEP uncertainty from the lidar one-year dataset (section 1.5.3.). The dark grey band indicates the interval [0.98, 1.02].

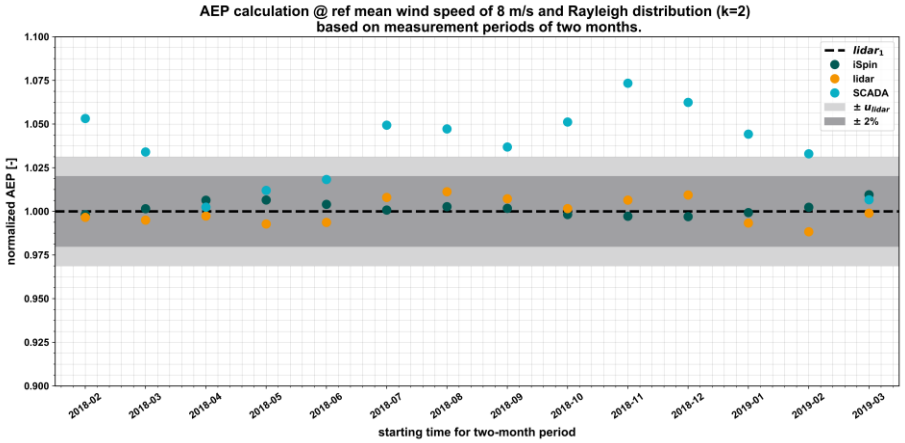

Figure 3 AEPs from the iSpin, lidar and nacelle anemometer (SCADA) power curves in two-month periods. Normalized by the AEP of the lidar one-year power curve (black dashed line).

1.5.3. SPINNER ANEMOMETER AND LIDAR AEP UNCERTAINTY

The AEP was calculated for the one-year lidar and spinner anemometer power curves for reference hub height annual wind speeds of 6m/s and 8m/s, with a Rayleigh probability density function [5]. The reference air density was 1.225kg/m^3. The results are shown in Table 3; the measured AEP values were normalized to the lidar AEP at the given speed.

Table 3 Measured AEP and uncertainty, from one-year dataset.

	V_{ave}= 6m/s		V_{ave}= 8m/s	
	Measured AEP, AEP_{meas}	Standard uncertainty in AEP, $u(AEP_{meas})$	Measured AEP, AEP_{meas}	Standard uncertainty in AEP, $u(AEP_{meas})$
Lidar	100.0%	4.8%· $AEP_{meas,lidar}$	100.0%	3.1%· $AEP_{meas,lidar}$
Spinner anemometer	99.9%	6.7%· $AEP_{meas,iSpin}$	100.0%	4.4%· $AEP_{meas,iSpin}$

1.6. STF SEASONALITY ANALYSIS

1.6.1. STF COMPARISON

The STFs obtained from the five datasets are shown in Figure 4. The first plot shows the wind speed difference $ws_{ref,n,i} - ws_{ispin,n,i}$, where "n" indicates the STF period (see Table 1), and "i" indicates the wind speed bin index. The second plot displays the difference relative to the one-year STF:

$$\Delta STF = \left(\left(ws_{ref,n,i} - ws_{ispin,n,i} \right) - \left(ws_{ref,1,i} - ws_{ispin,1,i} \right) \right) ws_{ref,1,i}^{-1}.$$

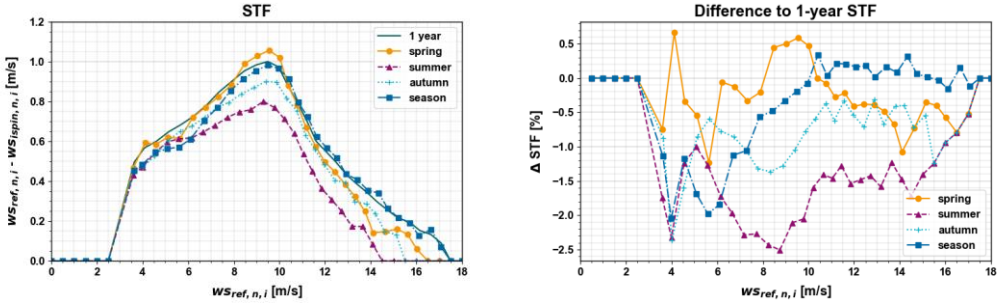

Figure 4 (Left) STFs from the five datasets. (Right) Wind speed difference between each two-month STF and the one-year STF. Reference speed is the lidar wind speed.

1.6.2. AEP COMPARISON

Next, we evaluated the difference in AEP due to the application of the season STFs, i.e. $STF_{n=2..5}$ (n=2..5), with respect to the application of the one-year function, STF_1. For each $STF_{n=2..5}$:

- we applied STF_n to the iSpin data,
- grouped the data in fourteen two-month datasets,
- calculated the iSpin power curve and AEP for each two-month dataset, $AEP_{n,m}$ (m=1..14).
- obtained the difference between the AEPs based on the season STF and the one-year STF: $\Delta AEP_{n,m} = (AEP_{n,m} - AEP_{1,m}) / AEP_{1,m} \times 100\%$.

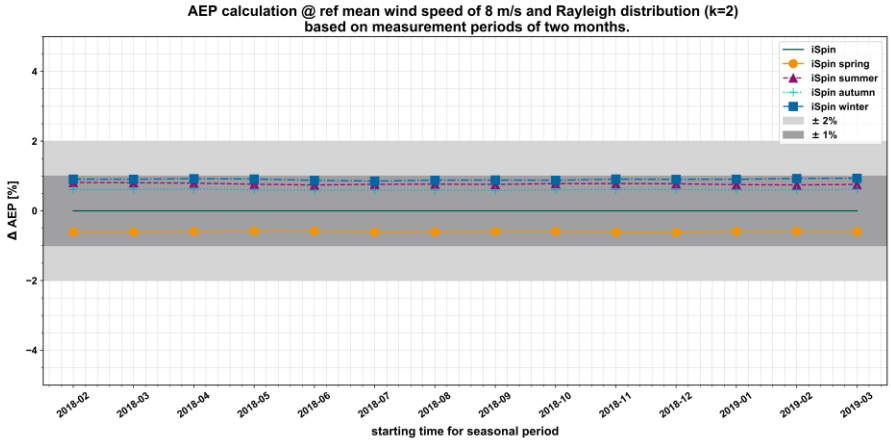

Figure 5 Difference between the AEPs based on the season STFs and the one-year STF, evaluated in two-month periods.

CONCLUSION

The analysis using a long-term STF showed that:

- The two-month-average wind speed differences between the spinner anemometer and the lidar were within ±2% of the reference wind speed, over a year.
- The spinner anemometer and lidar power curves and AEPs were consistent, considering their uncertainty intervals (calculated following IEC standards).
- The variation of the spinner anemometer and lidar AEPs during the year was lower than 1.6% of the lidar AEP.

The analysis using several STFs from different periods showed that:

- Differences between the one-year STF and the season STFs were within -0.5% and 2.5% of the reference speed.
- The AEPs from season STFs differed from the AEPs based on the one-year STF in less than 1%.

The seasonal robustness of the spinner anemometer measurements and the STF will be further investigated in PTP. The results presented and conclusion presented in this paper are preliminary, and may be revised at a later stage of the project.

ACKNOWLEDGEMENTS

The authors would like to thank EUDP for financing this research; the technical team in Romo Wind, DTU, and offshore site owner for the support provided regarding equipment installation; and the project partners for their feedback on the analysis inputs to the result discussions.

REFERENCES

1. https://www.ispin-ptp.com (accessed on 20th November 2019)
2. iSpin calibration procedures. ROMO Wind A/S. December 2018 (Version 12.0).
3. IEC TP61400 50-3 CD (May 2019)
4. IEC 61400-12-2 Ed1. 2013
5. IEC-61400-12-1 Ed2. 2017
6. Spinner Anemometer Uncertainty Analysis. TF Pedersen, P Gomez Arranz. DTU Wind Energy E-0166. April 2018.

CORRIGENDUM

The small differences between the plots presented in this paper and the plots included in the poster are due to the reprocessing of some datasets (seven weeks) to correct for an error in the timestamp alignment.